

NON-STANDARD METHODS OF DATA PROCESSING IN THERMOGRAPHIC NON-DESTRUCTIVE TESTING OF LIGHT BALLISTIC PROTECTIONS

Waldemar Świdorski

*Military Institute of Armament Technology
Wyszyńskiego Street 7, 05-220 Zielonka, Poland
tel.: +48 22 7641552, fax: +48 22 7641447
e-mail: waldemar.swiderski@wp.pl*

Marek Szudrowicz

*Military Institute of Armoured and Automotive Technology
Okuniewska Street 1, 05-070 Sulejówek, Poland
tel.: +48 22 6811025, fax: +48 22 6811073
e-mail: mszudrow@witpis.eu*

Abstract

IR thermography is a technique used to detection, registration, processing and visualization of invisible infrared radiation emitted by a tested object. Image (thermogram) is a result of this technique and it maps the distribution of temperature on surface of tested object. The image after entering in digital form into the computer needs to get certain treatments on it to separate information of interest through its processing. A characteristic feature of image processing is that the image exists at either the input or output of information processing. The output images should be free from disturbances and they should have distinctly separated features of interest. After the initial processing of the image, the next steps of its analysis follow. In the result of the analysis quantitative data is received that describes some determined features of the image and the complete image comprising hundreds details is substituted by a limited population of separated features. This population can be used effectively by different recognition methods and algorithms. In thermographic investigations, situations occur when treatment of images applied in standard software is not fully efficient to obtain information, which is "camouflaged" in taken thermogram. Such event takes place particularly in the case of looking for thermal "disturbances" onto the surface, which are caused by the undersurface defects. Such situation needs the application of special transformations carried out on thermograms. These transformations lead to selecting from all information included in the thermogram only such part of it that is essential from the point of view of conducted tests. In such case it is required the usage of advanced data processing techniques like thermal tomography, one-dimensional Fourier analysis, principle component analysis (PCA), an approximation by means of polynomials, wavelet analysis, neural network and reconstruction of thermographic signal. In this paper, these methods are described and examples of their use in tests of light ballistic protections are presented.

Keywords: *light ballistic protection, IR thermography, non-destructive testing, data processing*

1. Introduction

Composite materials have become recently very popular for making light ballistic protections. An interest in light ballistic protections results from threats which troops participating in stabilisation missions are exposed to. Usually they are equipped with motor vehicles exposed against small-calibre weapon fire and mine explosions. Therefore, it is necessary to provide an effective protection to these vehicles in order to guarantee an adequate safety level to their crews.

Due to the progress in polymer chemistry, it is currently possible to manufacture materials that provide an effective protection against small-calibre projectiles and shell fragments. Most often woven materials (fabric) are used and joined together by means of a plastic into multi-layer composite materials. They are used to manufacture personal ballistic protections (vests) as well as

armours for motor vehicles and fixed facilities. Composites of this kind are usually made from very strong aramid and polyethene fibres combined together by means of phenol or polyurethane resins or rubber mixtures. They can be also used in combination with steel metal sheets and ceramics to increase their effectiveness of protection against projectiles and fragments. Composite armours are easily replaceable and in case of damage, the damaged elements can be replaced by new ones without necessity of dismantling the whole cover. [1]

Considering the fact that light ballistic protections are usually several to more than 10-mm thick and are made of materials with thermo-physical properties, which are definitely different than those of potential defects that may occur in these materials the non-destructive testing by means of thermographic methods can be effective in detection of defects in them.

Thermographic non-destructive testing is not a new idea for assessment of materials. First tests in this area were performed at the break of the fifth and the sixth decade of the former century [2, 3]. However only after the development of capabilities of computer image analysis and appearance of thermal visualisation, systems of high resolution caused the application of non-destructive tests with usage of IR thermography by lifting considerably the range and quality of possible tests. The break of the XX-ith and the XXI-st century is symbolically represented by 2000 year, which is recognized as a very important period in IR technology development. The most practical event of that time was in appearance of commercial products – IR cameras with cooled focal plane array (FPA) detectors. Nowadays the IR thermal cameras are used as standard devices of NETD below 20 mK and possibilities of their usage in new applications considerably increased.

The usage of IR thermography is connected also with advantages and disadvantages of this technique.

The main advantages are:

- 1) Clear presentation of test results (colour thermograms).
- 2) High speed of testing (in comparison with other methods) that allows testing large area in relatively short time.
- 3) Suitable for various types of materials where defects show local changes of heat properties.

The disadvantages comprise:

- 1) High level of noises accompanying heat trial, especially disturbances connected with emissivity changes in absorption.
- 2) Strong dependence of detectability of the defect on defect size and depth of defect position under surface of tested material sample.
- 3) Short time of observation of changes, particularly during metals testing.

These disadvantages can be defeated or minimized through development and modernization of testing equipment and through development of new test procedures (data processing) and method of image (thermogram) analysis.

2. Thermogram Processing

Nowadays, the Pulsed Thermography is one of the most popular methods used in nondestructive tests of multi-layers composite materials. This type of material is usually used in light ballistic protections. Such tests are based on utilization of the lamp, laser and other devices to produce a pulse or a series of pulses of heating input which last from some milliseconds for the materials of high heat conductivity (e.g. for metals) to some seconds in the case of materials of small heat conductivity. Pulse cooling of the surface of the tested object (e.g. flow of cold air, liquid nitrogen etc.) can be also used. The Pulse Thermography can be realized by the reflection method or by transmission one and in general it provides a registered sequence of images (IR thermograms) with an identical time gap between the images. After switching off the heat, radiation source the tested object is cooled to ambient temperature. In the phase of cooling, the distribution of temperature on the surface of a tested object is measured and then this temperature distribution

is analyzed. Depending on heat parameters of tested material and on hidden defects existing inside it, the areas of higher and lower surface temperature appear indicating zones of possible material defects. To indicate more precisely the areas with defects usually special techniques of IR thermogram processing have to be utilized.

In thermographic investigations, situations occur when treatment of the images by tools of standard software is not fully efficient to obtain information, which is “camouflaged” in taken thermogram. It takes place particularly at looking for thermal “disturbances” onto the surface, which are caused by undersurface defects. Such situation needs the usage of special transformations of thermograms. These transformations allow selecting from all information included in the thermogram only such part of information that is essential from the point of view of conducted tests.

Image processing involves practically all world-known data processing algorithms. The most important algorithms are described below.

Temperature temporal evolutions in particular image pixels can be noisy. In order to smooth high-frequency noise, images processing enables applying a *fitting procedure* by using three different fitting functions.

The *first fitting function* (Fit 1) follows from the classical solution for heating a semi-infinite adiabatic body with a square pulse:

$$T(\tau) = A_0 + A_1 \theta + A_2 \theta^2 + A_3 \theta^3 + A_4 \theta^4 + A_5 \theta^5, \quad (1)$$

$$\theta = \sqrt{\frac{\tau}{\tau_h}} - \sqrt{\frac{\tau}{\tau_h} - 1}; \quad \tau \geq \tau_h,$$

where:

τ_h – the heating time,

T – temperature,

τ – time.

The *second fitting function* (Fit 2) is general and independent on the physics of the analyzed process:

$$T(\tau) = A_0 + A_1 \tau + A_2 \tau^2 + A_3 \tau^3 + A_4 \tau^4 + A_5 \tau^5. \quad (2)$$

The *third fitting function* (Fit 3) follows from the classical solution for heating a semi-infinite adiabatic body with a Dirac (flash) pulse:

$$\text{Ln}[T(\tau)] = A_0 + A_1 \Theta + A_2 \Theta^2 + A_3 \Theta^3 + A_4 \Theta^4 + A_5 \Theta^5, \quad (3)$$

$$\Theta = \text{Ln}[\tau].$$

Note that the Fit 1 (1) and Fit 2 (2) procedures are sensitive to values of all time parameters. The accurate knowledge of these parameters is advisable for obtaining better results.

Applying the above fitting functions results in calculating up to six *polynomial coefficients*: $A_0, A_1, A_2, A_3, A_4, A_5$. These coefficients are calculated for each image pixel (i, j) .

Choosing a particular fitting option depends on a source temporal function. The Fit 1 option is best applied to decaying temperature signals that take place after heating a sample during the τ_h time. The Fit 2 option can be used if temperature signals first grow up and then decay, thus participating in both a heating and cooling stage. The Fit 3 option, like the Fit 1 option, is typically applied to decaying temperature signals after flash (short pulse) heating. In the literature [4, 5], the Fit 3 fitting approach is often referred as the “*Log-Log*” signal presentation. In case of a semi-infinite body heated with a flash, the non-defect temperature evolution is represented by a straight line in the Log-Log presentation, thus facilitating discrimination of defect areas. This peculiarity of the Log-Log presentation is used in the synthetic data treatment approach patented by Thermal

Wave Imaging, U.S.A. In general, as mentioned above, the best results with the Fit 1 and Fit 2 functions will be obtained if a *true time* is prescribed to each image in a sequence by introducing the corresponding time parameters in the scenario.

The analysis of image sequences by applying the *Fourier transform* to the time coordinate allows producing phase images (phasegrams) which are characterized by enhanced signal-to-noise ratio compared to common amplitude images. The use of the two-dimensional Fourier transform enables the determination of material anisotropic thermal properties.

The Fourier transformation is applied to a whole image sequence (N images in a sequence) except the Image No. 1. If $T(i, j, k)$ is the temporal evolution in the pixel (i, j) , where $k = 2 \div N$ then 1D Fourier transformation is applied to pixel-based temporal evolutions of temperature signal in order to produce images of both magnitude and phase at different Fourier frequencies. The following of Fourier magnitudes and phases are used:

$$\begin{aligned} \text{Magnitude} &= \sqrt{[\text{Re}(T)]^2 + [\text{Im}(T)]^2} \\ \text{Phase} &= \text{ArcTan}\left[\frac{\text{Re}(T)}{\text{Im}(T)}\right], \end{aligned} \quad (4)$$

where $\text{Re}(T)$ and $\text{Im}(T)$ represents the real and imaginary part of the Fourier transform applied to the $T(i, j, k)$ function.

It is important that results of the Fourier transformation at particular frequencies depend on the number of images in a sequence and on whether the background (first) image was subtracted from the sequence or not. Images of phase (phasegrams) are typically preferable in regard to images of magnitude. It is often believed that phasegrams are able to underline the subtlest differences between the temperatures in a defect and non-defect area. All Fourier images can be produced at a chosen frequency. Low-frequency Fourier images are preferable. However, this Fourier transformation peculiarity does not affect much the discrimination between *non-defect* and *defect* areas in the Fourier transforms. The interpretation of Fourier images is typically done *qualitatively*. In many cases, the *first non-zero* Fourier frequency provides optimal results because with higher frequencies noise grows up.

The Fourier transformation of temporal evolutions is used in the Thermal NDT technique called *Pulse Phase Thermography (PPT)* [6, 7]. Usually, the Fourier transformation is fulfilled in order to obtain *images of phase (phasegrams)* that are assumed to be less sensitive to surface noise than source IR images. Some Thermal NDT experts believe that phasegrams taking into account quite subtle differences in signal temporal evolutions ensure the *best visibility* of subsurface defects. Therefore, the time-domain Fourier transformation of image sequences is often regarded as the technique No. 1 in transient Thermal NDT.

In Thermal NDT, normalization often allows significant suppression of the noise caused by uneven heating. This algorithm involves division of each image in the current sequence by a chosen image $T_{norm}(i, j, \tau_{norm})$ called *normalizing*.

The general formula of the normalization is:

$$C_{norm}(i, j, \tau) = \frac{T(i, j, \tau)}{T_{norm}(i, j, \tau_{norm})}, \quad (5)$$

where C_{norm} is the *normalized contrast* (specified below as simply C unlike the *running temperature contrast* C^{run} introduced below) and τ_{norm} is the time at which a normalizing image is chosen.

The *correlation* technique is intended for revealing similarity in the temporal behaviour of the temperature between a chosen reference point and each image pixel. A reference point is to be chosen by the User. Then the correlation image will show pixel-based values of the correlation coefficient $r(i, j)$ according to the following formula:

$$r(i, j) = \frac{\sum_{k=1}^N T(i, j, k)T(i_{ref}, j_{ref}, k) - \frac{1}{N} \sum_{k=1}^N T(i, j, k) \cdot \sum_{k=1}^N T(i_{ref}, j_{ref}, k)}{\sqrt{\left\{ \sum_{k=1}^N T^2(i, j, k) - \frac{1}{N} \left[\sum_{k=1}^N T(i, j, k) \right]^2 \right\} \cdot \left\{ \sum_{k=1}^N T^2(i_{ref}, j_{ref}, k) - \frac{1}{N} \left[\sum_{k=1}^N T(i_{ref}, j_{ref}, k) \right]^2 \right\}}}, \quad (6)$$

where $T(i, j, k)$ is the pixel value in the k -th image and $T(i_{ref}, j_{ref}, k)$ is the pixel value in a reference point and N is the number of images in the sequences except the first one.

The correlation technique has not been much used in Thermal NDT and its potentials need further exploration. Our experience shows that in some cases this technique allows the efficient suppression of uneven noise and emissivity phenomena. Note that, due to a great deal of time points involved into consideration, correlation coefficients are often close to unity. A spread in $r(i, j)$ values between a defect and non-defect area can be enhanced by choosing shorter time intervals where temperature deviations caused by defects are observed best of all.

Principal component analysis is a novel statistical technique intended for processing raw data represented as three-dimensional vectors, e.g. image sequences. This technique allows sorting out raw data in such way that the most significant image properties will be contained in few first images of the-so-called principal components, thus ensuring efficient reduction of information redundancy.

Wavelet analysis is a type of integral transforms of which the core is represented with some special functions called ‘wavelets’. Wavelets are basis functions, which meet some specific requirements and enable data scaling by space and time. Sometimes, the wavelet method is called ‘mathematical lens’ due to its feature to analyze both large and small signals.

Neural networks are regarded as an element of artificial intelligence. They are constructed by using elementary cells called neurons. By proper network training, it is possible to identify and classify raw data; in NDT, this is equivalent to defect detection and characterization respectively.

Thermal tomography means ‘slicing’ a sample for in-depth layers where the distribution of thermal properties can be visualized, by analogy with X-ray tomography. Thermal tomography is accomplished by analyzing the temperature evolution on the surface of a component to be inspected, following an initial thermal stimulation. Such stimulation can be realized by applying pulse heating with pulse duration ranging from a few milliseconds for high-conductivity materials (metals) to a few seconds for low-conductivity materials (composites). It is important that thermal stimulation be supposed to be nondestructive, i.e. not to damage a test material due to overheating. Dynamic temperature signals, which appear on the surface of test samples, are recorded with an infrared camera. Technically, any thermal tomography procedure represents the corresponding standard procedure of thermal nondestructive testing. In fact, a key point in performing thermal tomography is a data processing algorithm, which is supposed to convert the so-called *heat transit times* into material layer coordinates. Such an algorithm is to be applied to a captured image sequence where defect indications evolve in time. The important feature of DTT is the necessity of choosing a ‘non-defect’ *reference point*, in regard to which heat transit times are analyzed.[8]

In this study, two approaches to thermal tomography have been explored. The first approach is “classical”, thus involving into consideration a reference point. The second approach can be called ‘no-reference tomography’ because it does not require introducing any specific reference point. This can be done in a two-fold way. First, the temperature behaviour in non-defect points can be modelled by using some solutions, which are well known in the heat conduction theory. Second, the polynomial fitting of different orders can be applied to all pixel functions assuming that non-defect evolutions are ‘smooth’ while defect evolutions reveal some perturbations, which should appear in high-order polynomials. The idea of such tomography was suggested by Vavilov [9] and in this study, we shall explore it.

In Thermal NDT, statistical data treatment enables *quantitative* comparison of test procedures and processing algorithms. For example, the results of applying processing algorithms to a particular set of experimental data can be *ranged* by signal-to-noise (SNR) ratio values, thus allowing the choosing of optimum algorithms.

The experimental part of the work has been performed on a sample made of Carbon Fibre Reinforced Plastic. The sample contained 25 square Teflon inserts placed between different composite plies (Fig. 1). The test sample by the size of 300x300x2 mm was made of 10-ply CFRP composite and contained 25 Teflon square-shaped inserts (lateral size 3, 5, 7, 10 and 15 mm) at various depths: 0.2, 0.4, 0.6, 0.8 and 1.0 mm.

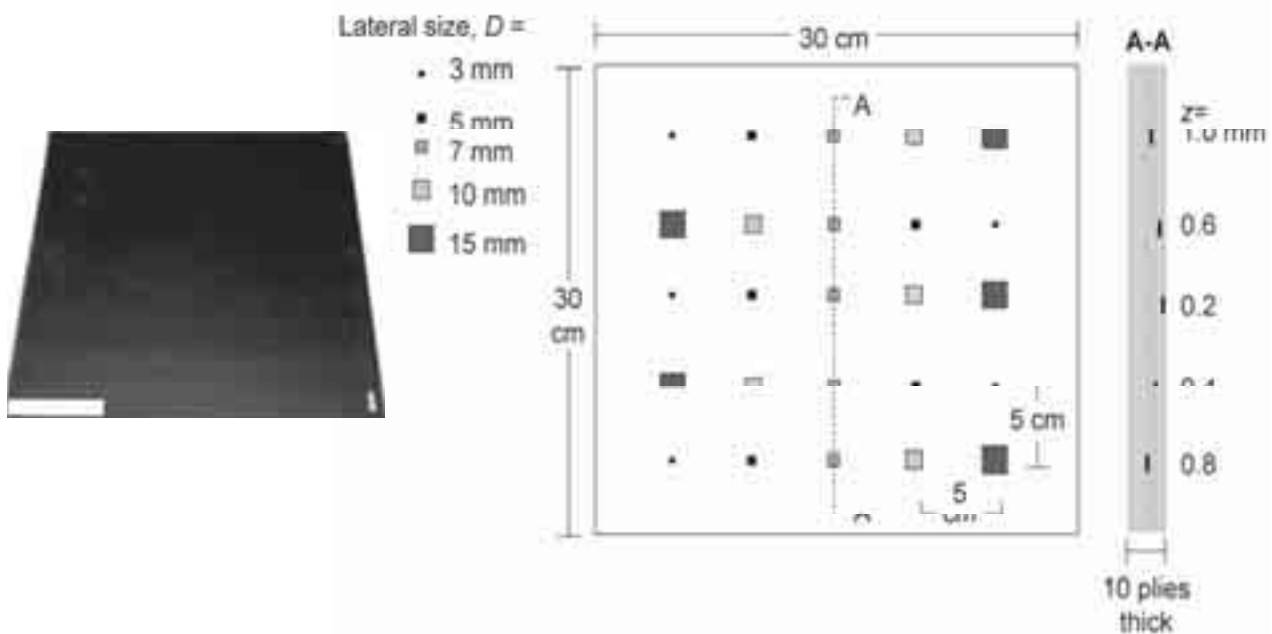


Fig. 1. Standard specimen of 10-layer carbon plastic 2 mm thick (25 flaws in the form of Teflon inserts)

To optimize the algorithm for processing experimental data we chose a signal-to-noise ratio (SNR) for defect *A* (Fig. 2a) (at a depth of 1 mm, with a size of 15 × 15 mm) calculated with respect to a neighbouring point selected as a reference one. It was established that the optimal initial image was characterized by SNR ~ 1 (Fig. 3a). The normalization of data that involves division of all thermograms in the sequence by a chosen image, which contains no marks from flaws, considerably reduces the effect of non-uniform heating (compare the thermograms in Figs. 2a and 3a) and leads to SNR = 2.7 (Fig. 2a). The maximum SNR = 9.5 was observed in the image of the second principal component (Fig. 2d). It was revealed that, in contrast to the well-known phase data processing, which usually improves the “visibility” of all hidden flaws, the principal-component method has a tendency for emphasizing certain flaws, and it is difficult to determine beforehand what kind they are. This feature of the PCA method is illustrated in Fig. 2d, where all flaws at a depth of 0.4 mm produce rather weak marks. In this case, the limiting possibility of the PCA method is characterized by a flaw of 5 × 5 mm detected at a depth of 1 mm [14].

Some preliminary results of dynamic thermal tomography (“no-reference” approach) which are shown in Fig. 4 demonstrate that the visibility of defects within particular layers can be enhanced in regard to the “classical” algorithm of thermal tomography. For example, the tomogram in Fig. 4a exhibits two defects instead of three defects in the tomogram of Fig. 3g. In addition, the image in Fig. 3b is much better than its “classical” counterpart in Fig. 3h because it contains no artifacts.

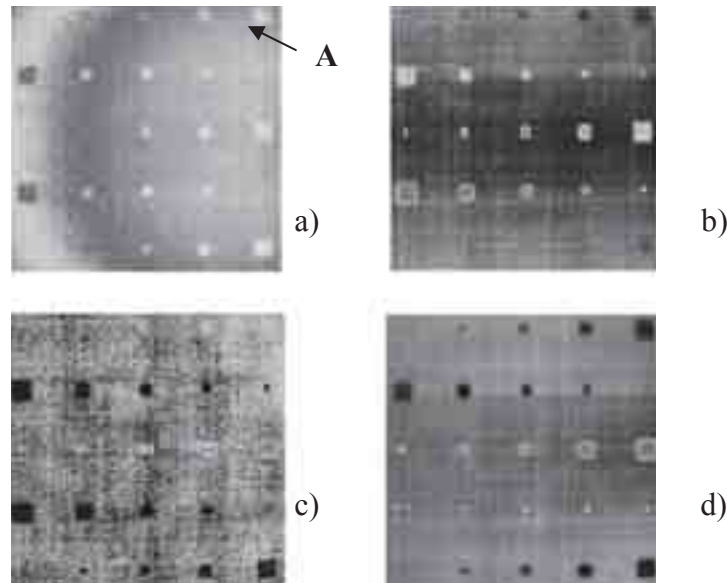


Fig. 2. Selection of an optimal algorithm for processing the results of TT of a carbon plastic specimen (Fig. 1): (a) optimal initial image after normalization (SNR = 2.7); (b) phasogram (SNR = 3.9); (c) "optimal" polynomial coefficient (SNR = 0.9); and (d) second principal component (SNR = 9.5)

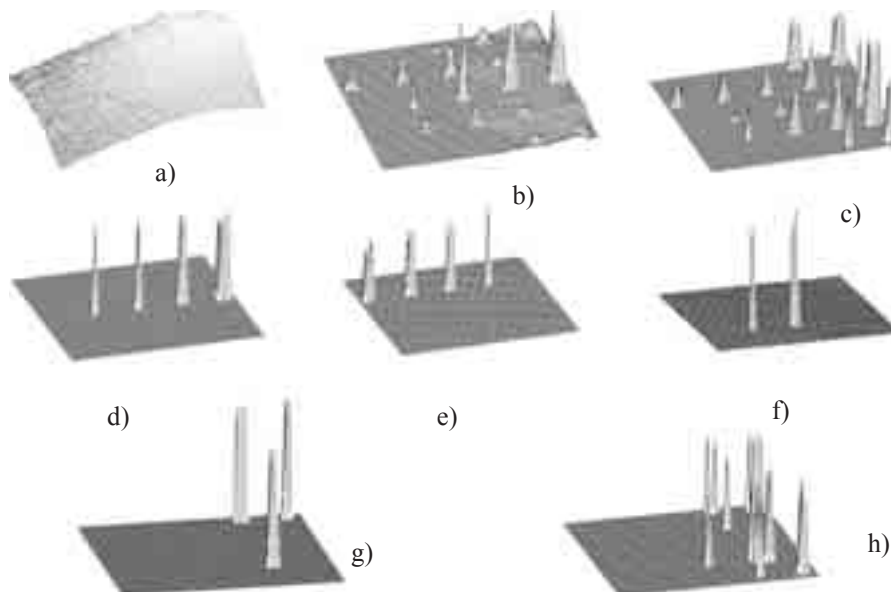


Fig. 3. Tomographic analysis of a carbon plastic specimen (Fig. 2): (a) optimal initial image (SNR = 1.0); (b) maxigram; (c) timogram; (d) thermal tomogram of a layer of 0.24–0.31 mm; (e) tomogram of a layer of 0.42–0.54; (f) tomogram of a layer of 0.60–0.66 mm; (g) tomogram of a layer of 0.67–0.69 mm; and (h) tomogram of a layer of 0.71–0.83 mm

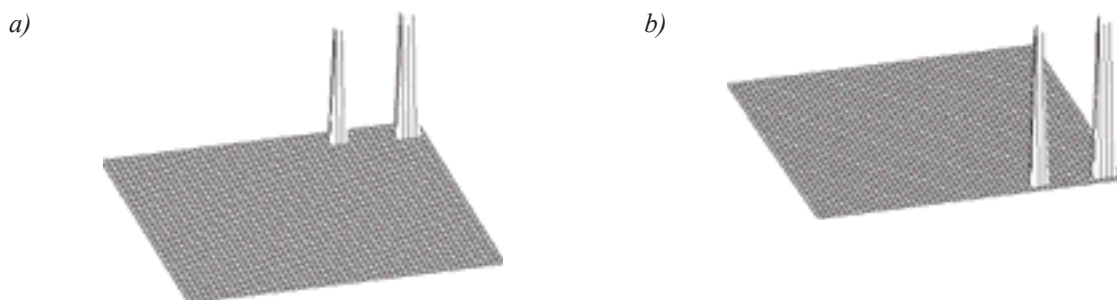


Fig. 4. "No-reference" thermal tomography algorithm: a - thermal tomogram (layer 0.70-0.73 mm), b - thermal tomogram (layer 0.76-0.90 mm)

3. Lock-in Thermography

The set-up for experimental testing with Lock - in method is presented in Fig. 5. The thermal wave is generated by a heat source, which is a lamp of about 1 kW power. The heat source is calibrated by the Lock - in Module, which provides sinusoidal form of thermal wave at specific frequency [11-13].

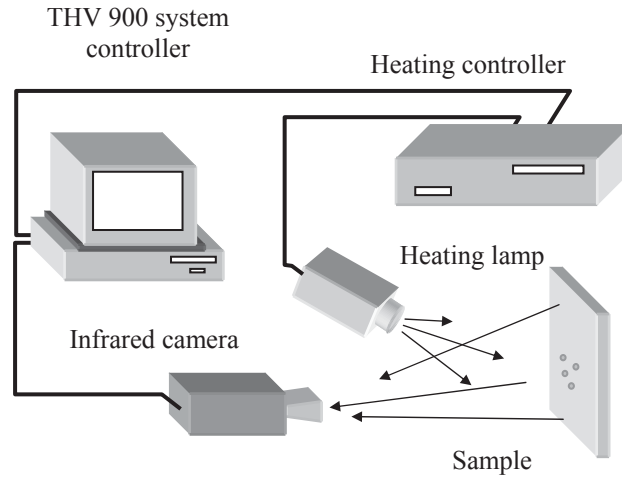


Fig. 5. Experimental set-up

In order to get interference images the THV 900 System Controller collects the series of images to compare their temperature, calculate amplitude, and phase angle of imaging thermal wave in every point of the image. Amplitude and phase images are not disturbed by secondary radiation from the surface of testing object. The phase image is undisturbed by differences in emissivity of the surface and non-uniform distribution of heat emitted by the source.

The system Lock - in divides each cycle of the thermal wave on four equal parts (Fig. 6) and collects an equal number of images in each part. Images from each part are averaged to produce four images with averaged signal values of thermal camera S_1 , S_2 , S_3 , S_4 .

The phase and amplitude is then calculated for each pixel of the image according to following equations [7, 8]:

$$\varphi = \arctan\left(\frac{S_1 - S_3}{S_2 - S_4}\right), \quad (7)$$

$$A = \sqrt{[S_1 - S_3]^2 + [S_2 - S_4]^2}. \quad (8)$$

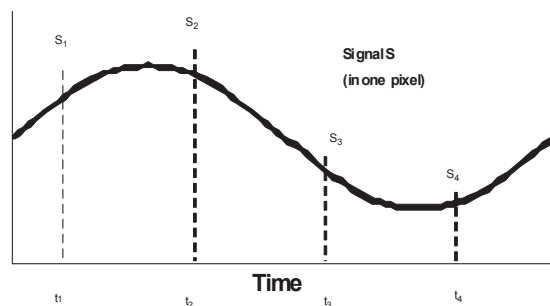


Fig. 6. Signal acquisition during thermal wave cycle

Figure 8 shows exemplary phasograms of the aramid laminate (Fig. 7), presenting internal damage of the laminate structure on both the projectile entry side (Fig. 8a) and the exit side (Fig. 8b). The damage area was determined as a diameter of a circle that contained internal damage of the material caused by an impact of the projectile shot at the sample. Fig. 10 presents exemplary phasograms of the glass fibre laminate (Fig. 9), showing visible subsurficial damage on both the projectile entry and exit sides. Prior to the non-destructive tests, all samples underwent destructive tests using the V_{50} method.



Fig. 7. Sample of the 6-layer aramide laminate after V_{50} destructive tests.

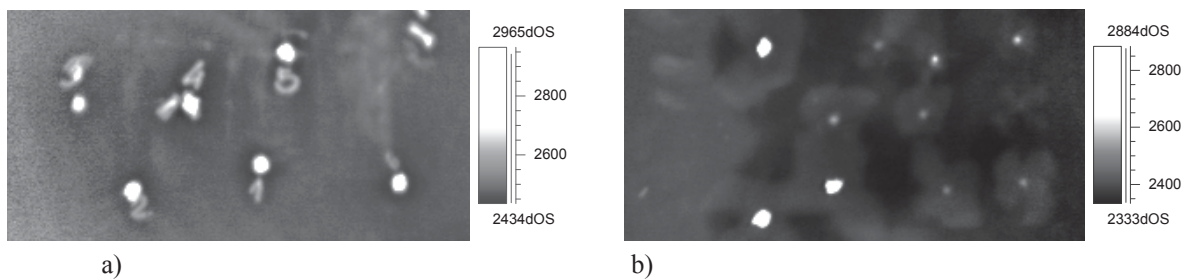


Fig. 8. Phasograms (0.04 Hz) of the aramid fibre laminate: a) on the impact side, b) on the other side



Fig. 9. Sample of the 15-layer glass fibre laminate after V_{50} destructive tests

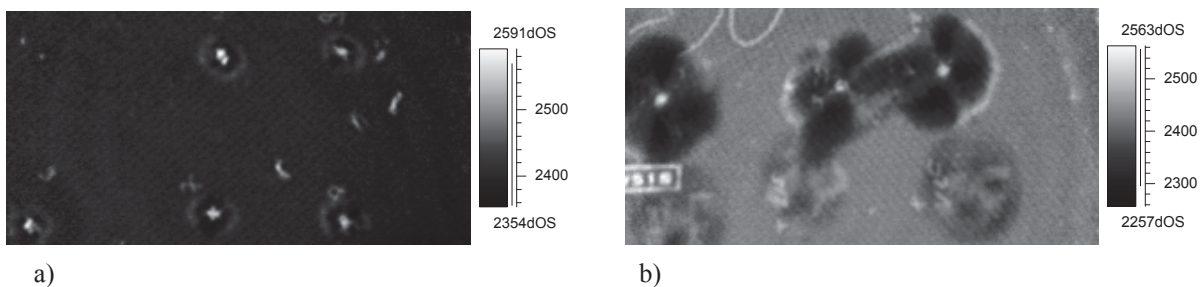


Fig. 10. Phasograms (0.04 Hz) of the glass fibre laminate: a) on the impact side, b) on the other side

4. Conclusions

It was shown in the paper that pulsed thermography and optical lock-in thermography are interesting methods for detection of defects (destruction area) in light ballistic protections made of multi-layer composite materials.

In many cases of the pulsed method, it is necessary to use an algorithm analysis of thermograms to detect defects (e.g. Normalization, Polynomial Fitting, Thermal Tomography, Principal Component Analysis and Correlation Analysis etc.). This allows on precise analysis of tested structure of composites but it usually is time-consuming. The use of optical lock-in thermography method shortens time testing though this method can be less precise in cases of detecting small and deeply located defects.

Optical lock-in thermography method can be very useful to evaluation of light ballistic protections after destructive testing of the V_{50} ballistic limit method.

The authors of paper think that the development of IT will bring some new data processing methods, which will make possible to get out the information about defects considerably below level of noises than it is possible so far.

References

- [1] Świdorski, W., Szabra, D., Vavilov, V., *Modeling defects in polyaramide composite material*, VII Krajowa Konferencja TTP'2006, pp. 109-113, Ustroń 2006.
- [2] Florant, L. E., *Testing using infrared*, J.Am. Instrum. Soc., 11, p. 61, 1964.
- [3] Beller, W. S., *Navy sees promise in infrared thermography for soild case checking*, Missiles and Rockets, 16, p. 22, 1965.
- [4] Shepard, S., *Advances in Pulsed Thermography*, Proc. SPIE "Thermosense XXIII, Vol. 4360, pp. 511-515, Orlando 2001.
- [5] Shepard, S., Lhota, J. R., Hou, Y., Ahmed, T., *Gold Standard Comparison of Thermographic Sequence Data*, Insight, Vol. 46, No. 4, pp. 210-213, 2004.
- [6] Maldague, X., Marinetti, S., *Pulse phase infrared thermography*, *J. Appl. Phys.*, Vol.79, pp. 2694-2698, 1996.
- [7] Couturier, J.-P., Maldague, X., *Pulsed phase thermography of aluminum specimens*, Proc. SPIE "Thermosense-XIX", Vol. 3056, pp. 170-175, Orlando 1997.
- [8] Świdorski, W., *The characterization of defects in multi-layered composite materials by thermal tomography methods*, Acta Physica Polonica A, Vol. 115, No. 4, pp.765-769, 2009.
- [9] Vavilov, V., *Thermal nondestructive testing*, Handbook series "Nondestructive testing", Mashinostroyenie Publish., Vol. 5, p. 380 , Moscow 2006.
- [10] Wu, D., Busse, G., *Lock-in thermography for nondestructive evaluation of materials*, Revue Generale de Thermique, Vol. 37, No. 8, , pp. 693-703, 1998.
- [11] Świdorski, W., *Lock-in Thermography to rapid evaluation of damage area in composite materials used in military application*, SPIE, Vol. 5132, pp. 506-517, 2003.
- [12] Habaj, W., Świdorski, W., *Thermography-Applications to the Testing of Bullet Protection and Ballistic Limit v 50 for Composite Armours Based on Reinforced Plastics* QCAV'2001, pp. 49-53, Le Creusot 2001.
- [13] Świdorski, W., Hłosta, P., Szudrowicz, M., *Nondestructive testing of multi-layer composites made of carbon fibre by pulsed IR thermography*, PAK, Vol. 55, No. 11, pp. 906-909, 2009.
- [14] Vavilov, V., Nesteruk, D., Shiryayev, V., Ivanov, A., Świdorski, W., *Thermal (infrared) tomography: Terminology, principal procedures, and application to nondestructive testing of composite materials*, Russian Journal of Nondestructive Testing, Vol. 46, No. 3, pp. 151-161, 2010.